- Technical Paper -

EVALUATION ON THE LONGITUDINAL BAR PULL-OUT EFFECT OF A RC COLUMN BASED ON E-DEFENSE EXCITATION

Heng GAO[*1], Kenji KOSA[*2], Tatsuo SASAKI[*3] and Zhongqi SHI[*4]

ABSTRACT

Displacement of RC column, which is not only caused by flexure but also rotation induced by longitudinal bar pulling out from inside footing. To evaluate the effect of pulling out of the longitudinal bar (pullout) in the column top displacement, experimental data of a full-scale RC column (C1-1) by shake table test is summarized. Pullout at base contributes about 33.6% to the column top displacement. Analysis was conducted to explain the mechanism of pullout. The experimental and analytical results showed that multi-layer induced reduction influence from bar-to-bar contributes to pullout.

Keywords: E-Defense excitation, pulling out, strain distribution, multi-layer, bar-to-bar reduction

1. INTRODUCTION

A 3D shake table experiment on a large-scale reinforced concrete bridge using E-Defense has been constructed by the National Research Institute for Earth Science and Disaster Prevention. With the facilities for E-Defense, a series of anti-seismic experiments of bridges has been conducted, among which a full-scale RC column named C1-1 [1] has been constructed. To study the mechanisms of flexural failure for large-scale reinforced concrete columns representing typical columns built in the 1970s, the first shake table experiment based on C1-1 was conducted in Dec. 2007.

C1-1 is a specimen that was designed for evaluating flexural failure. Response displacement of an RC column, which contributes to the development of lateral displacement of the deck, is not only caused by flexure but also rotation induced by the longitudinal bar pulling out from the inside footing. It is defined hereinafter as pullout. A few researches have paid attention to this pullout, including different methods to calculate it. In the shake table experiment of C1-1, the displacement meter (LVDT) at the base and the strain gauge (SG) attached on the longitudinal bars are referred to for measuring the pullout displacement.

As the SG is much more sensitive than LVDT, experimental data by LVDT is summarized firstly in Chapter 3. Moreover, to reveal the actual effect of pullout on response displacement of the column top, the part of the pullout induced column displacement is solved. In order to clarify the mechanism of pullout, measured data by SG is summarized and analysis is conducted in Chapter 4. In former research [2], theoretical calculation methods have been raised. The results of experiments and analysis clarified that the multi-layer (tri-layer in C1-1) induced bar-to-bar reduction influence contributes to pullout.

2. EXPERIMENTAL SETUP

As mentioned in Chapter 1, C1-1 is a specimen that was designed to be subject to damage by flexural moment. In this chapter, the setup of C1-1 will be explained in detail.

As Fig. 1 shows, the column was constructed by tri-layer of reinforcement of 29mm diameter, 32, 32 and 16 bars at outer, middle and inner layers respectively. Deformed circular stirrups of 13mm diameter are provided at 300mm intervals. At the top zone of 1.15m and at the base zone of 0.95m length, outer ties are provided at 150mm intervals. Stirrups are lap spliced at 390mm. The longitudinal reinforced ratio was 2.02%, and the tie volumetric reinforced ratio for the middle was 0.32% and for the top or base was 0.42%. On the day of the experiment, the yield strength of the longitudinal bars, stirrups and concrete were measured as 366 MPa,

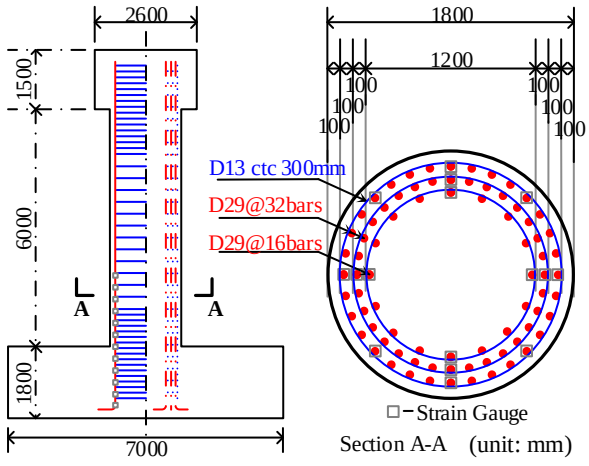

(a) Side View (b) Sectional View

Fig. 1 C1-1 Column on E-Defense

*1 Graduate Student, Graduate School of Engineering, Kyushu Institute of Technology, JCI Student Member
*2 Ph.D., Prof., Department of Civil Engineering, Kyushu Institute of Technology, JCI Member
*3 M. of Eng., Manager, Technical Generalization Division, Nippon Engineering Consultants Co., Ltd.
*4 Ph.D. Candidate, Graduate School of Engineering, Kyushu Institute of Technology, JCI Student Member

193 MPa and 33 MPa. Evaluation of C1-1 based on JRA 2002 was conducted, and the yield and ultimate displacement results in 0.046 m and 0.099 m respectively (δ_y = 0.046 m, δ_u = 0.099 m).

Strain gauges were attached to the longitudinal bar shown in Fig. 1 and provided at 300 mm intervals. In both the transverse and bridge axis direction, the SG was attached to the outer, middle and inner bar as shown in Fig. 1(b). As for the displacement meter at base, shown in Fig. 2, the series of LVDT was set at the base by both sides of the transverse and bridge axis direction. The first meter was set at 80mm height and the others are provided at 200 mm intervals and 10 units of meters were set at the base of each side.

Footing of C1-1 was fixed on shake table of E-Defense. The table was excited using E-Takatori ground motion which was about 80% amplitude of the original motion (Takatori ground motion). Main excitation using 100% E-Takatori ground motion was conducted twice.

3. MEASURED PULLOUT DISPLACEMENT

This chapter summarizes the experimental data. The column top displacement was measured by three-dimensional displacement meter (LVDT) attached to the column top. Experimental data for pullout, which causes the column base rotation, was measured by LVDT at base. To reveal the actual effect of the pullout on column top displacement, the part of displacement caused by pullout inside footing was solved.

3.1 Response Displacement of Column Top

Experimental data based on the column top was plotted initially by the load-displacement (P-δ) relationship in Fig. 3. The maximum load was about 1390 kN and 1660 kN respectively in the bridge axis (East-West) and the transverse (North-South) direction. In transverse and bridge axis directions, column displacement exceeded $2\delta_y$ and $3\delta_y$.

The response displacement orbit of the column top (7.5m from the base of the column) is illustrated in Fig. 4. As the column top keeps displacing in the two-dimensional area shown in Fig. 4, the response displacement in the bridge axis direction and the transverse direction will be discussed respectively. According to Fig. 4, taking the northward displacement as an example firstly, when the response displacement towards the north direction reach $1\delta_y$ by the first time, the absolute displacement of the column top towards north corresponds to the one-dimensional axis of north-south and marked as N1. Then, when the column displacement of northward reaches $2\delta_y$ by the first time, the absolute displacement towards north corresponds to the one-dimensional axis of north-south and marked as N2. Similarly, when the column displacement reaches certain $n\delta_y$ towards each direction by the first time, the absolute displacement of column top corresponds to the one-dimensional axis and marked by different character respectively. In bridge axis and transverse direction, the absolute displacement of column top in each one-dimensional axis exceeded $3\delta_y$ and $2\delta_y$ respectively.

The response displacement of column top, as it is

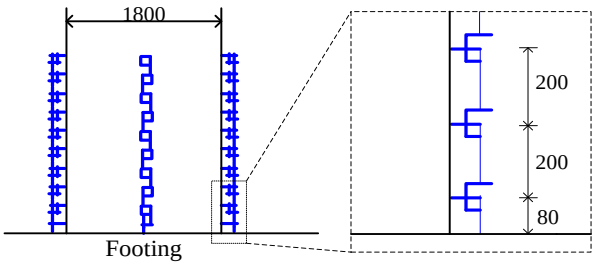

Fig. 2 Set of displacement meter

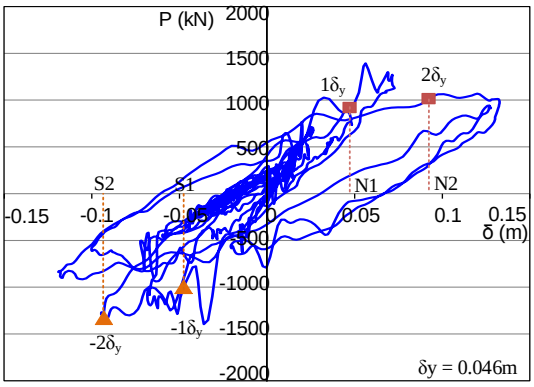

(a) Transverse direction (North-South)

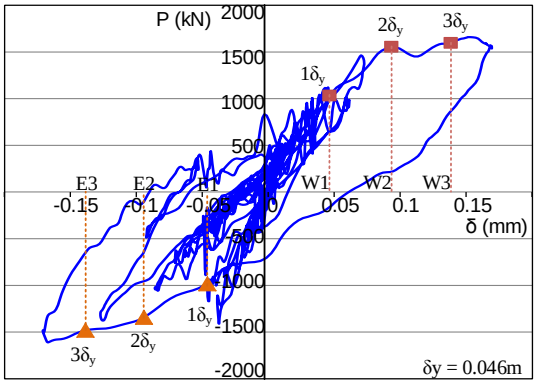

(b) Bridge axis direction (East-West)

Fig. 3 Load-Displacement relationship of top

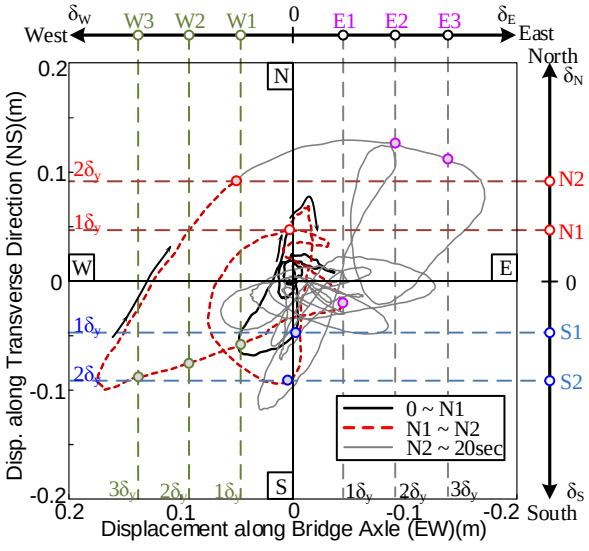

Fig. 4 Displacement orbit of top point

stated above, is not only caused by flexure but also base rotation induced by longitudinal bar pulling out from footing. Consequently, base rotation induced column displacement should be distinguished to reveal the actual effect of pullout. Fig. 5 is plotted to explain the procedure for solving the part of column displacement caused by pullout. Bridge axle and transverse direction are discussed separately during the evaluation of pullout.

Firstly, when the displacement of column top reaches $1\delta_y$ towards north marked as N1, the corresponding pullout displacement (the same time as N1) at south side is marked as u_{s1} (s: south; 1: $1\delta_y$), which is obtained from the experimental data by the LVDT of 80mm height at base shown in Fig. 2. Secondly, neutral axis, marked as X_0 in Fig. 5 (b), is solved by the cross-section calculation with analytical tools SUCCESS. Thirdly, with the measured pullout (u_{s1}) and neutral axis (X_0), base rotation can be solved ($\tan\theta = u_{s1} / X_0$). Finally, as Step 4 shown in the flow, the part of column displacement caused by pullout can be solved by the base rotation and height of column ($\delta_{N1\text{-pullout}} = u_{s1} / X_0 \times 7.5$ m). The ratio of pullout induced column displacement ($\delta_{N1\text{-pullout}}$) takes in the total one (δ_{N1}) is solved to reveal the actual effect of pullout at base.

3.2 Measured Pullout by Displacement Meter

According to the step 1 in Fig. 5, measured pullout displacement history is initially plotted in Fig. 6 (a) and (b) respectively for north - south side and east - west side. In Fig. 6, as the meters at compression side has been very sensitive, only the experimental data at the certain side acting as extension is plotted. As illustrated in Fig. 6 (a), measured u_{s1} reaches 1.95 mm. Similarly, the corresponding pullout displacement at each side is marked as u_{ij} (i stands for 'direction' = n, s, e, w; j stands for 'times' of δ_y = 1, 2, 3) in Fig. 6 (a) and (b) according to the response column displacement referring to Fig. 4.

Based on the history in Fig. 6, Fig. 7 makes a general summary of the pullout displacement at the just point ($n\delta_y$) of response column displacement. Except the west side, which is seriously damaged at base leading to the measured data being unreasonable, the other three sides are gathered in the Fig. 7. Characters (e.g. u_{s1}) have also been marked in Fig. 7 corresponding to Fig. 6. Shown in Fig. 7, the pullout displacement increases gradually along the top displacement increases and the data of north and south roughly accord.

As shown in Fig. 7, at column displacement of $1\delta_y$, the measured data at east side is relatively greater than that of north and south sides with same absolute displacement towards the corresponding direction. This difference can be explained by the actual location of column top illustrated in Fig. 4. According to the orbit of the column top, W1 is located S-W area so that the measured u_{e1} not only includes the pullout caused by top displacement of $1\delta_y$ towards west but also that caused by top displacement towards south (about $1.3\delta_y$). However, as for N1, it is located approximately on the north-south axis so that the measured pullout displacement u_{s1} is only caused by the top displacement of $1\delta_y$ towards north. Although N1 and W1 have same absolute displacement on the one-dimensional axis, the actual measured u_{e1}

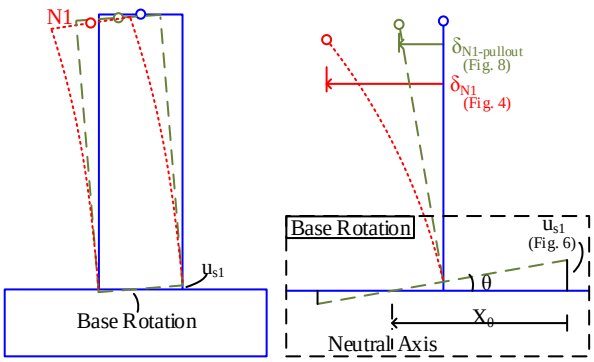

(a) Measured data about pullout

1 Pullout Displacement (u_{s1}, Fig. 6)
↓
2 Location of Neutral Axis (X_0)
↓
3 Base Rotation (θ)
↓
4 Displacement due to Pullout ($\delta_{N1\text{-pullout}}$, Fig. 8)
↓
Effect of Pullout at Base ($\delta_{N1\text{-pullout}}/\delta_{N1}$, Fig. 9)

(b) Study flow

Fig. 5 Measured data and study flow

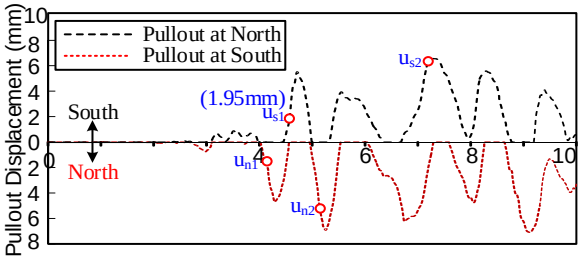

(a) Pullout displacement history at North and South

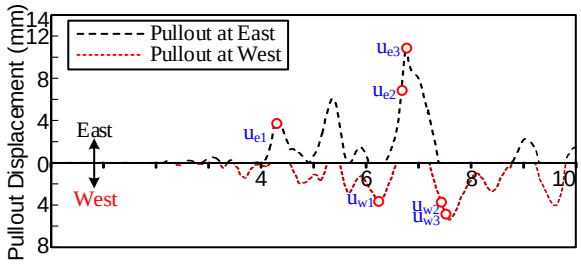

(b) Pullout displacement history at East and West

Fig. 6 Measured pullout displacement history

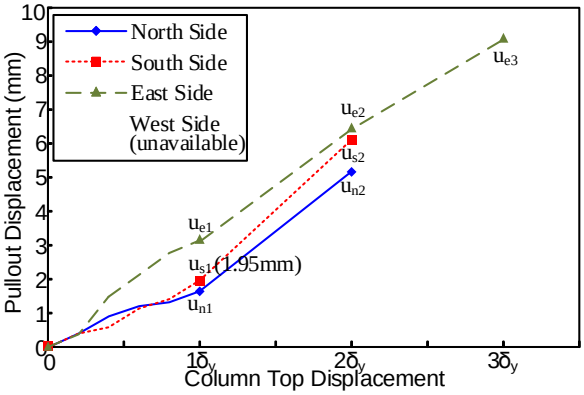

Fig. 7 Pullout displacement at certain $n\delta_y$

consists of this two parts of value leading to its value being relatively greater than that of north and south side, and the experimental data is reasonable.

According to the methods illustrated in Fig. 5, based on the measured pullout displacement shown in Fig. 7 and calculated location of neutral axis, the base rotation (u_{s1}/X_0) can be solved and pullout induced column displacement ($\delta_{N1\text{-pullout}}$) can be distinguished from the response column displacement (in Fig. 4, δ_{N1}). Fig. 8 is plotted to make a general summary about the part of column displacement caused by pullout. The location of the neutral axis for certain column displacement can be extrapolated by the linear relationship from δ_y ((δ_y, X_{0y}) = (0.046m, 0.93m)) to δ_u ((δ_u, X_{0u}) = (0.099m, 1.42 m)) which is solved from the cross-section calculation. Taking the N1 as an example, the measured pullout displacement is u_{s1} (= 1.95mm) and neutral axis is X_0 (= 0.93m). Column displacement caused by pullout at south side (u_{s1}) marked as $\delta_{N1\text{-pullout}}$ in Fig. 8 is calculated as 0.013m ($\delta_{N1\text{-pullout}} = u_{s1} / X_0 \times 7.5$m). Similarly, the part of column displacement caused by pullout at different side can be solved in Fig. 8.

According to Fig. 8, which distinguishes the displacement caused by pullout from the response column displacement, Fig. 9 reveals the actual effect of the pullout at base by plotting the ratio of the induced displacement in response to the displacement of column top. As explained above, the actual measured u_{e1} consists of this two parts of value leading to its value being relatively greater. The ratio of column displacement caused by this pullout (u_{e1}) is relatively higher shown in Fig. 9. Column displacement of $3\delta_y$ (0.138 m) exceeded the ultimate displacement (δ_u = 0.099 m), and the used location of neutral axis at ultimate state may not be accurate leading its lower ratio at $3\delta_y$. As shown in Fig. 9, ignoring the data by east side at $1\delta_y$ which is much greater, pullout at base has contributed 33.6% to the top displacement on average during $1\delta_y \sim 3\delta_y$. Consequently, the pullout cannot be neglected and its mechanism should be discussed further with the experimental data measured by SG on longitudinal bars inside the footing.

4. EVALUATION OF MEASURED DATA BY STRAIN GAUGE

4.1 Experimental Data by Strain Gauge

Based on the measured data by LVDT in Chapter 3, pullout contributed to the response column displacement by 33.6% which is relatively great. In this chapter, the mechanism of pullout is evaluated based on experimental data and analysis.

As for the experimental data by SG, Fig. 10 is plotted to illustrate the strain history measured by outer bar at south side for an example. The data measured by SG at 0 m and -0.3 m are shown in Fig. 10. Corresponding to the column displacement, for example, the $\varepsilon_{1\text{-}0}$, in which 1 stands for times of δ_y ($n\delta_y$) and 0 stands for the measured strain at 0 m, is marked by the same time when column displacement reaches yield displacement ($1\delta_y$). Similarly, the other measured data by SG at just point of $n\delta_y$ are found and marked in the history. As the strain gauge at compression side is very

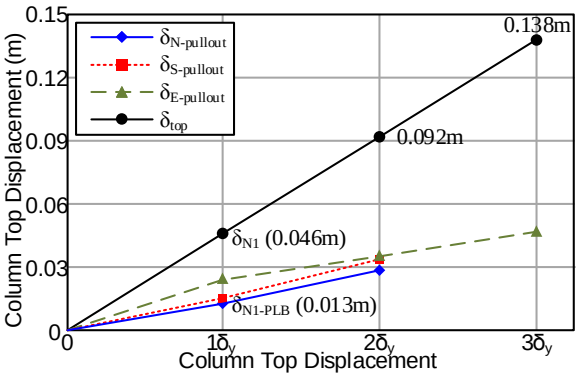

Fig. 8 Column top displacement due to pullout

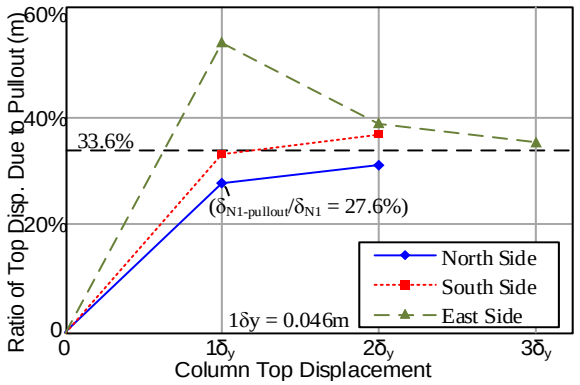

Fig.9 Ratio of top displacement due to pullout

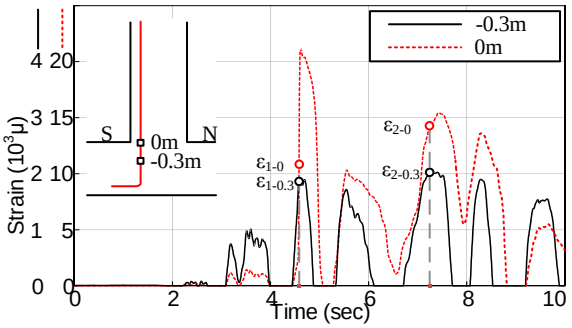

Fig.10 Strain history of outer bar (South)

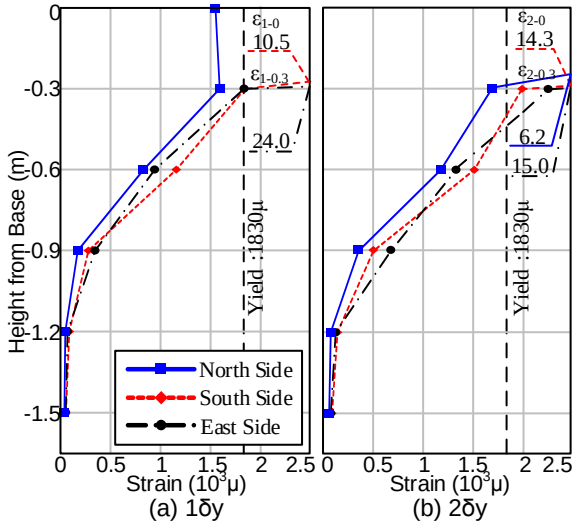

Fig.11 Strain distribution measured by SG (Outer)

sensitive, only the data at tension side is plotted in Fig. 10. Besides, the strain distribution along the longitudinal bar inside the footing (from -1.5 m to 0 m) has been plotted in the Fig. 11 with the experimental data of -0.3 m and 0 m in Fig. 10. The distribution can be generally divided into two parts, below and upon -0.3 m. The measured strain distribution of each side below -0.3 m roughly accords with each other at certain $n\delta_y$, however, the data upon -0.3m shows a great difference. At height of -0.3 m, strain of south and east side has exceeded yield strain (1830μ) at both $1\delta_y$ and $2\delta_y$ respectively shown in Fig. 11 (a) and Fig. 11 (b). Moreover, as shown in Fig. 11, the strain at base (0 m), which reaches 10500μ and 14300μ respectively at $1\delta_y$ and $2\delta_y$, has greatly increased from the data at -0.3 m. It can be found that strain of -0.3 m ~ 0 m determines the pullout of longitudinal bar.

4.2 Analysis on the Pullout

Analysis is conducted based on the calculated methods reported in the literature [2]. The following theoretical equation shows the relationship of bond stress, steel stress and slip (τ-s and σ-τ):

$$\tau / f_{ck}^{'} = 0.73(\ln(1+5000S/\phi))^3/(1+\varepsilon\times10^5) \quad (1)$$

$$\Delta\sigma = \pi\cdot\phi\cdot\Delta x\cdot\tau/A_s \quad (2)$$

Here, τ is the bond stress between concrete and steel bars; f'_{ck} is compressive strength of concrete; S is bond slip; ϕ is the diameter of longitudinal bar; ε is strain; Δσ is the increment of stress in interval of Δx.

Based on the equations listed above, the analytical procedure can be shown as the flow in Fig. 12. Firstly, the strain of longitudinal bar at base (0m) is defined according to the experimental data. For example, when the column top displacement reaches $1\delta_y$ (0.046m) the measured strain by SG at base is 10497μ so that in analysis the strain at base (0m) is defined as 10497μ for the state of $1\delta_y$. Secondly, assume a certain value for the pullout at base and use it to make calculations based on Eq. (1) and (2) shown in Fig. 12. The analysis results in the series of stress, strain and corresponding pullout displacement according to the Step 3, Step 4 and Step 5 in the Fig. 12. Thirdly, judgment is made on the bond slip at the end of steel. When the analytical bond slip at the end of longitudinal bar is not zero, the former assumed pullout at base should be reset and the same analysis conducted again as shown in Fig. 12 (a). The analysis can come to an end until the bond slip at the bottom of longitudinal bar in analysis is zero.

With the analysis shown in Fig. 12, the analytical results on pullout displacement and strain distribution along the longitudinal bar inside the footing can be solved. This kind of analysis, defined hereinafter as Case 1, has been conducted by considering a single bar inside footing, however, the C1-1 has been reinforced by tri-layer which may contribute to the reduction influence from bar-to-bar. Another modification [3] considering this part of reduction, defined hereinafter as Case 2, has been conducted. The calculated method for reduction coefficient for bond stress and slip relationship (τ-s) can be shown as follows:

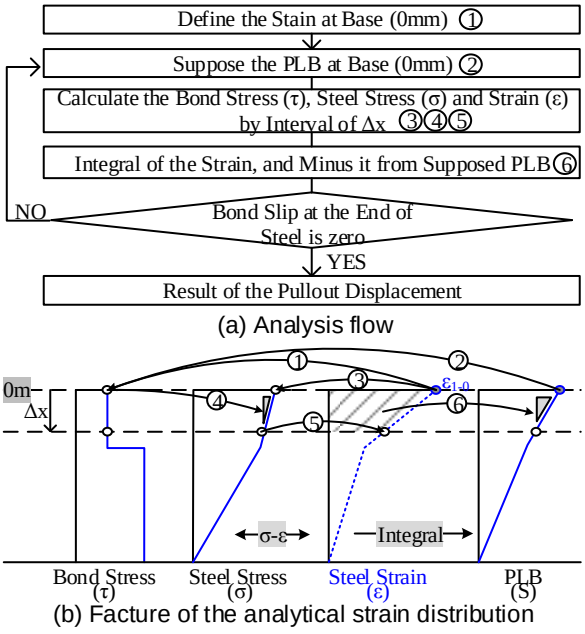

Fig.12 Analysis flow

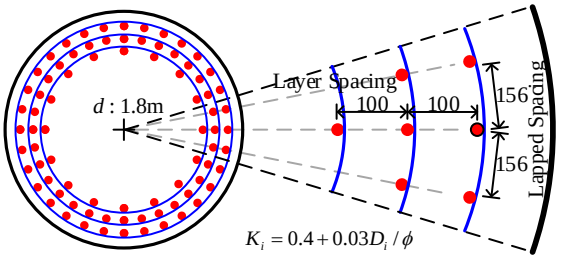

Fig.13 Reduction coefficient

$$K_i = 0.4 + 0.03D_i/\phi \quad (3)$$

Here, the D_i is the distance between two adjacent bars and ϕ is the diameter of longitudinal bar.

The reduction coefficient for bond stress can be calculated based on the Fig. 13. One of the bars in outer layer is taken as an example, the maximum distance of layer spacing is 100mm and it is 156mm for lapped spacing. Based on Eq. (3), the component reduction coefficient can be calculated as 0.503 and 0.561 respectively. As for the reduction coefficient of bond stress, it is defined as product of calculated component value by both lapped and layer spacing which is calculated as 0.282 (0.503 × 0.561). Based on Eq. (1), analysis that bond stress multiplied by the reduction coefficient of 0.282 is conducted according to the analytical flow in Fig. 12.

4.3 Analytical Results

The analytical results are plotted in Fig. 14 based on the analytical model explained in Section 4.1, in which the (a) and (b) illustrate the state of column displacement at $1\delta_y$ and $2\delta_y$. According to Fig. 14 (a) and (b), when the column displacement reaches $1\delta_y$ and $2\delta_y$, the analytical result of strain in analysis of Case 2 has reappeared the experiment better than the analysis of Case 1. As it stated above, the C1-1 specimen is constructed by tri-layer of reinforcement. In order to evaluate the effect of multi-layer, depth of bond fracture

and analytical pullout displacement at base is discussed based on the analytical result plotted in Fig. 14.

According to the referenced research [3], when the bond slip (S in Eq. (1)), which is integrated from the strain distribution, exceeds 0.014ϕ (= $0.014 \times 29 = 0.406$ mm), it is defined as the beginning of bond fracture depth. Based on analytical result, at $1\delta_y$, bond fracture occurs from -0.465 m and -1.419 m to the base (0 m) respectively for Case 1 and Case 2 analysis. At $2\delta_y$, it is at -0.494 m and -1.449 m depth respectively for Case 1 and Case 2 analysis. By the comparison between Case 1 and Case 2, multi-layer of reinforcement have caused the bond fracture to begin deeper inside the footing which may lead pullout at base to become greater.

At $1\delta_y$ of column displacement, pullout at base, shown as the table in Fig. 14 (a), is integrated as 2.59 mm and column displacement caused by pullout takes 48% of the response column displacement. Analysis of Case 1 and Case 2 results in 0.66 mm and 2.18 mm respectively. Column displacement caused by pullout takes 12.6% and 40% of the response column displacement respectively for Case 1 and Case 2. Similarly, as for state of $2\delta_y$ shown in Fig. 14 (b), pullout displacement is results in 3.4 mm in experiment by SG which contributes to the response column displacement by 22%. In analysis, pullout is got as 1.03 mm and 3.52 mm respectively for Case 1 and Case 2 analysis. The ratio of column displacement caused by pullout reaches 7% and 23% respectively for Case 1 and Case 2.

Analytical pullout and column displacement caused by pullout in Case 2 analysis is on average 3.3 times greater than that in Case 1 analysis. Considering both lapped spacing and layer spacing in reduction coefficient, Case 2 analysis has well reappeared the experiment. It is clarified that multi-layer of reinforcement (tri-layer in C1-1) has caused bond fracture to begin deeper leading pullout at base becoming greater. With the relatively great pullout, column displacement caused by pullout shows a relatively high ratio (33.6% averagely) in the response column displacement of experiment.

5. CONCLUSIONS

Based on the experiment and analysis on C1-1, the actual effect of pullout at base on response column displacement and its mechanism were evaluated, following conclusions have been drawn:

(1) Specimen C1-1 is an RC column constructed by full-scale and tri-layer reinforcement. After the first excitation experiment of C1-1, displacement of column top exceeded $2\delta_y$ (0.092m) in both north and south direction and exceeded $3\delta_y$ (0.138m) toward both east and west directions. Due to the relatively greater displacement toward north-east direction actually, base of the south-west side was seriously damaged.

(2) Data measured by the displacement meter at base corner is defined as the pullout displacement of longitudinal bar (pullout). It is measured as 1.95 mm and 6.05 mm at south side respectively in $1\delta_y$ and $2\delta_y$. Pullout displacement keeps increasing along the column top displacement increase. Base rotation, which is caused by the pullout and can be solved by the pullout and corresponding location of neural axis, has contributed to the response displacement of column top by 33.6%.

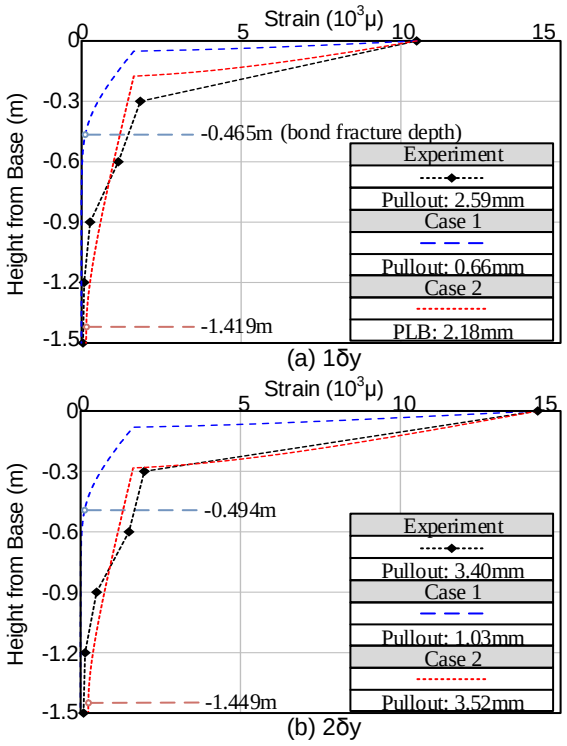

Fig.14 Experimental and analytical result

(3) Analysis considering the bar-to-bar reduction with close lapped spacing and layer spacing has well reappeared the experiment. In analysis considering the reduction influence, bond fracture depth is solved as -1.419 m and -1.449 m respectively at $1\delta_y$ and $2\delta_y$, which is much deeper than that in analysis just considering single bar. As bond fracture beginning deeper in analysis considering bar-to-bar reduction, the analytical pullout increases by 3.3 times on everage over that in the analysis only considering single bar. Multi-layer of reinforcement (tri-layer in C1-1) contributes to great pullout and leads the column displacement caused by pullout to take a relatively higher ratio in the response column displacement of experiment.

REFERENCES

[1] Ukon, H., et al.: Large-scale Shake Table Experiment on a Component Model (C1-1 model) Using E-Defense, Technical Note of The National Research Institute for Earthquake Science and Disaster Prevention, No.331, 2009

[2] Chou, L., et al.: Bond Characteristics in Post-yield Range of Deformed Bars, J. of JSCE, No.378/V-6, pp.213-220, 1987.2

[3] Ishibashi, C., et al.: Study on Deformation Capacity of Reinforced Concrete Bridge Piers under Earthquake, J. of JSCE, No.390/V-8, pp.57-65, 1988.2